PRECISE ATOMIC MASS DETERMINATIONS OF THE STABLE ISOBARIC TRIPLET ^{124}Sn - ^{124}Te - ^{124}Xe

by

Bernard Joseph Hall

A thesis

presented to the University of Manitoba

in partial fulfillment of the

requirements for the degree of

Master of Science

in

Department of Physics

Winnipeg, Manitoba

October, 1983

PRECISE ATOMIC MASS DETERMINATIONS OF THE STABLE ISOBARIC TRIPLET

^{124}Sn - ^{124}Te - ^{124}Xe

by

Bernard Joseph Hall

A thesis submitted to the Faculty of Graduate Studies of
the University of Manitoba in partial fulfillment of the requirements
of the degree of

MASTER OF SCIENCE

MASTER OF SCIENCE (1983)
(Physics)

UNIVERSITY OF MANITOBA
Winnipeg, Manitoba

TITLE: PRECISE ATOMIC MASSES OF THE STABLE ISOBARIC TRIPLET ^{124}Sn - ^{124}Te - ^{124}Xe

AUTHOR: Bernard Joseph Hall, B.Sc.(Hons)

SUPERVISOR: Dr. R. C. Barber

NUMBER OF PAGES: v, 61

CONTENT AND SCOPE:

Using the "Manitoba 2" high resolution double focusing mass spectrometer, precise atomic mass determinations were performed on the stable isobaric triplet at mass number A=124 (^{124}Sn-^{124}Te-^{124}Xe), the $^{54}Fe^{35}Cl_2$ ion (A=124), and the $^{13}C^{37}Cl_3$ ion (A=124). A total of eight measurements were carried out, 4 being absolute atomic mass measurements (measurements made relative to $^{13}C^{37}Cl_3$) and 4 being relative atomic mass measurements. Measurements between the $^{54}Fe^{35}Cl_2$ compound, ^{124}Xe and ^{124}Te provide an important and unusual link across the mass table of 70 mass units. The results obtained provide significantly better values for the double beta-decay energies at this mass number. As well, the precision of the ^{124}Xe mass was improved substantially.

ACKNOWLEDGMENT

This research was supported by the National Science and Engineering Reasearch Council.

There are many whom I would like to thank for their help and guidance without which I would never have completed this work. Among these are my parents, for doing what parents are supposed to do, Dr. R. C. Barber, for revealing to me and guiding me in the "art" of Mass Spectrometry, and Dr. H. E. Duckworth for his guidance and insight.

This acknowledgment would not be complete without mention of the members of the Mass Spec Group whose assistance was invaluable. This includes Dr. Kumar Sharma, Ron Ellis, Gary Dyck, Cliff Lander and Paul Beaudoin.

Finally, this thesis was completed in spite of Gary.

TABLE OF CONTENTS

List of Figures

List of Tables

Chapter 1

A History of Mass Spectrometry

1.1 INTRODUCTION

Mass Spectrometery finds its roots in the late nineteenth century. The discovery by Goldstein (1886) of 'positive rays' laid the foundation for J.J. Thomson's future work (1913) into positive ray parabolas. Utilizing equipment first developed by Kaufman (1901), Thomson was able to distinguish, for the first time, evidence for isotopes amongst the stable elements.

The limitations of the positive ray method were soon recognized and, as a result, different methods for separating chemical species according to their isotopic constituents were soon developed. One such developement was Aston's "Mass Spectrograph". He used both electric and magnetic fields, arranged to cause deflection in opposite directions, so as to obtain a velocity focused beam, i.e. all ions of a particular e/m ratio, regardless of their velocity, would arrive at the same detection point. The apparatus did not however, posses direction focusing, i.e. ions diverging from the optic axis did not return to a focus. Careful collimation was used in order to keep image

broadening small. Using this machine Aston obtained further evidence of the isotopic composition of elements, most notably for the elements Neon and Chlorine.

At about the same time similar work was being done by A.J. Dempster. His equipment differed considerably from that being used by Aston. Dempster employed a magnetic field which acted on the ion beam over 180 degrees. This arrangement provided for direction focusing, i.e. monoenergetic ions of a given e/m which diverge at 0 degrees will come together at 180 degrees. By varying the accelerating potential different e/m groups were brought to the collector. Dempster provided information on Mg, Li, Ca and Zn.

Further work on similar apparatus was done by K.T. Bainbridge (1933). He introduced a velocity filter to the input of his machine so as to eliminate the previously required monoenergetic source. The most significant contributions made by Bainbridge were in the light mass region including investigations into heavy hydrogen, lithium and helium. Work was also done on the elements Zn, Ge and Te.

One might note from the preceding discussion that, up to 1933, 'mass analyzing apparatus' fell into two distinct categories, viz. either direction or velocity focusing. Clearly it is desirable that an instrument have both properties and thus, having just one, left these machines severly limited. This

realization led to the development of the 'double focusing instrument' which possesses both.The idea dates back to Dempster (1929) but it was not until 1934 when Herzog completed a mathematical analysis of the problem , presenting general equations governing the passage of ions through electric and magnetic field combinations, that work began on such an instrument. The first such machine was completed by Dempster in 1935 and others soon followed. In the subsequent years major advances were made in precise atomic mass determinations. The high resolving power of double focusing instruments allowed for the separation of isotopes and contaminants thereby facilitating the measurements of relative and absolute masses and abundances of the isotopes of elements throughout the periodic table.

To this point the discussion has centred around 'deflection-type' instruments. It must be noted that other types of instruments have also been developed and have found applications in many areas of physics and chemistry. Among these are the 'Time of Flight' instruments, the 'Mass Synchrometer', 'Quadrupole' mass spectrometers and 'Ion Cyclotron Resonance' machines.

Time of flight apparatus utilizes the fact that ions of different masses, falling through a given potential, will take varying times to traverse a straight beam tube. This technique is currently being exploited for the analysis of large molecules which would otherwise be broken up in the source of a deflection

type instrument (Standing et al., 1982).

The mass synchrometer, primarily developed by L.G. Smith (1956),exploites the dependence of the cyclotron frequency on mass. Ions are contained within a homogeneous magnetic field and are hence forced to travel in circular paths. The circulating ion beam can be modulated in velocity with an r.f. voltage, which is at a multiple of the cyclotron frequency and is applied to a set of beam defining slits. Thus, a given mass, which is selected by the r.f. voltage, will travel along a unique path. Ions with different masses will travel along other paths and are not allowed to reach the detector, this being accomplished by the use of narrow slits and baffels. This type of spectrometer was used exclusively for atomic mass determinations and formed the basis for an advanced version, currently at the University of Technology in Delft (Koets, 1981).

Quadrupole mass spectrometers, on the other hand, have proven to be very popular. A quadrupole field is set up (often by four cylindrical electrodes) with both d.c. and a.c. components. Ions passing through this region begin to oscillate but only ions of a given mass, proportional to the a.c. and d.c. frequency combination, will pass through the device. Relatively simple construction, small size and the low energy requirement for the ion beam (a few eV) make quadrupole instruments highly desirable for many applications. A major drawback is their fairly low resolving power, less than 1/1000.

Finally, a variety of quadrapole ion traps have been constructed (Dawson, 1976). Of special interest, because it has been demonstrated to be capable of resolving powers of up to $1/10^8$, is the fourier transform ion cyclotron resonance (FTICR) mass spectrometer. The ions to be analyzed are contained within a small cell which itself is contained inside a homogeneous magnetic field. The ions, which are either produced inside (or introduced into the cell), are excited with an r.f. field. The circulating ions then produce an a.c. signal on two detecting plates inside the cell. Each mass present produces a signal having a characteristic frequency and the fourier transform of the sum of these reveals a mass spectrum. Though still in the developement stages, this type of instrument shows great promise. It has the capability of very high resolving power while requiring as few as 100 ions to operate.

1.2 Contributions to Nuclear Physics

Precise atomic mass determinations have proven invaluable to nuclear physics. Much about nuclear structure can be deduced from atomic mass information, such as closed shells, changes in shape, and pairing of nucleons. The mass difference between neighboring isotopes, for instance, is directly related to the binding energy of the last nucleon. Atomic masses are also directly related to the energy release involved in a nuclear reaction. Also,

predictions of the original shell model failed to account for closed shell effects (experimental) at the 'magic' nucleon numbers 28, 50, 82, and 126. A modification was then forced upon the theory in the form of an additional spin-orbit coupling. Because nuclear mass plays this important role attempts have been made to construct semi-empirical mass formulae, these being useful for extrapolation or interpolation into regions of the mass table where experimental data is not available. Of these attempts several have met with varying degrees of success. These include approaches which fit the experimental mass data to smooth curves so that extrapolations may be made, to attempts which derive the mass from more fundamental considerations as in the Hartree-Fock and Nilson-Strutinsky methods. Another, and remarkably successful formula, is the isobaric multiplet mass equation, which gives values with uncertainties as low as 40 keV (Midstream adjustment, see Maripuu, 1975).

1.3 Atomic Mass Table

Atomic mass data, which has been collected for several decades now, has been set out in an Atomic Mass Table. Since the number of measurements made far exceeds the number of nuclides the mass of each can be subject to least squares adjustment. Such a method was set up by Mattauch (1969). This has been used and the 1977 mass table (Wapstra and Bos, 1977) includes adjusted values

for available data.

1.4 Decay and Reaction Methods

Finally, a discussion of atomic mass measurement would not be complete without the inclusion of the Alpha Decay, Beta Decay and Nuclear Reaction methods for atomic mass determination.

A typical alpha decay may be written as:

(1-1) $${}_{z}M^{A}c^{2} \longrightarrow {}_{z-2}M^{A-4}c^{2} + {}_{2}He^{4} + Q$$

where Q is the total energy released. Since the ${}_{2}He^{4}$ mass is very well known, the unknown mass can be determined by an evaluation of Q. Q is most accurately determined using magnetic analysers or, to lesser accuracy, semiconductor detectors are also employed. Uncertainties for these measurements range usually from 2 to 50 kev, but in some cases as low as or lower than .5 keV.

Beta decay schemes follow three forms:

(1-2) $${}_{z}M^{A}c^{2} \longrightarrow {}_{z+1}M^{A+}c^{2}(\text{positive ion}) + mc^{2} + Q$$

(1-3) $${}_{z+1}M^{A}c^{2} \longrightarrow {}_{z}M^{A-}c^{2}(\text{negative ion}) + mc^{2} + Q$$

(1-4) $${}_{z+1}M^{A}c^{2} \longrightarrow {}_{z}m^{A}c^{2}(\text{neutral but excited}) + Q$$

Here, Q represents the change in mass. The first two of the above equations can be rewritten as follows:

(1-5) $$Q = {}_{z}M^{A}c^{2} - {}_{z+1}M^{A}c_{2}$$

(1-6) $$Q = {}_{z+1}M^{A}c^{2} - {}_{z}M^{A}c^{2} - 2mc^{2}$$

Thus, with one mass known, a measurement of Q_{B+-}, using a beta ray spectrometer, gives the unknown mass. For the electron capture mode we can get:

(1-7) $$Q_{ec} = {}_{z+1}M^{A}c^{2} - {}_{z}M^{A}c^{2}$$

where Qec shows up as the difference in binding energy between parent and daughter plus neutrino energy plus recoil energy. The final result is most often a burst of X-rays produced by cascading electrons. The energy of these X-rays is measured and a mass difference is thus obtained.

Finally, we come to nuclear reactions, generally given in the form:

(1-8) $$a + X \longrightarrow Y + b + Q$$

Knowing the masses of a and b and with a measurement of Q, the X-Y mass difference can be extracted.

The most precise mass measurements of this type are done using an (n, γ) reaction, giving uncertainties in the 0.5 kev range. Other reactions used for mass measurement are (γ,n), (d,p), (t,p) and (d,t).

Chapter 2

Ion Optics

Double focusing in a deflection-type instrument is achieved by subjecting the ion beam to both electric and magnetic fields. For an ion of charge q and mass m travelling with a velocity v perpendicular to a magnetic field B, we have the following:

(2-1) $$r_m = m\dot{v}/qB$$

where a is the radius of curvature of the ions trajectory. Similarly, for an ion traversing an electric field we get:

(2-2) $$r_e = 2kmv^2/qV$$

with the electric field being given by:

(2-3) $$E \approx V/2k$$

here V is the plate potential, the plates having radii a+k and a-k such that $k \ll a$.

In order to see clearly how double focusing comes about we shall look first at the field sectors separatly.

From Herzog's work (1934) we have, first, for monoenergetic ions diverging at most from the optic axis with a half angle spread alpha:(refer to Fig. 2-1)

(2-4) $$f=r_m/\sin\phi_m$$

(2-5) $$(l_m'-g_m)(l_m''-g_m)=f^2$$

(2-6) $$g=f_m\cos\phi_m$$

Next, for an ion traversing the same magnetic field with conditions changed from equation (2-1) above to: $m=m(1+\delta)$ and $v=v(1+\beta)$, where $\delta,\beta<<1$, and taking a displacement b_m of the object into account we get(using the notation of Sharma , 1979):

(2-7) $$b_m'=r_m(\beta+\gamma)B_1-b_mB_2$$

where B_1 and B_2 are constants depending upon the geometry of the machine.

Similarly, for radial electrostatic fields Herzog arrived at: (refer to Fig. 2-2)

(2-8) $$(l_e'-g_e)(l_e'-g_e)=f^2$$

(2-9) $$f=r_e/\sqrt{2}\sin\sqrt{2}\phi_e$$

(2-10) $$g=f\cos\sqrt{2}\phi_e$$

(2-11) $$b_e=r_e(\beta+1/2\gamma)E_1-b_eE_2$$

In the above discussion we have set β to be a small change in velocity above or below the given velocity v. Note that in equation (2-) the coefficients for γ and β are the same, whereas in equation (2-1) they are different. This allows us to construct an ion path through both electric and magnetic field regions in such a manner that the β coefficient vanishes yet leaving a finite value for γ. This leaves us with an instrument which has no velocity dispersion while at the same time maintaining mass dispersion. More explicitly, combining equations (2-6) and (2-10) gives:

(2-12) $$b'=(r_mB_1-1/2r_eE_1B_2)+(r_mB_1-r_eE_1B_2)+bE_1B_2$$

If we set:

(2-13) $$r_mB_1=r_eE_1B_2$$

we arrive at the desired condition.

It must be stressed at this point that a number of assumptions were made in the preceding discussion. We did not take into account the fringing fields of both the electric and magnetic sectors. Neither did we account for oblique entry, into the field regions, of ions travelling along trajectories off the optic axis. The latter case has been taken into account by more general expressions of Herzog (1934). Hintenberger and Konig (1959) first gave expressions to describe focusing for geometries to second order, while detailed descriptions of the effect of fringe fields have been given by Coggeshall (1947), Bainbridge (1949, 1953), Ploch and Walcher (1950), Reutersward (1951, 1952), Barnard (1953, 1958), Konig and Hintenberger (1955), Herzog (1955), Enge (1964), Baril and Kerwin (1965) and Ezoe (1970).

Herzog's work provides us with a number of important relationships. From equation (2-11) we can call the coefficient of the mass dispersion D and the coefficient of b the magnification M. It is easy to see then, that the image width W can be given as:

$$W = Ms_0 \tag{2-14}$$

where s_0 is the object slit width. This is the case for photographic detection where no image broadening is attributed to the detection method. In the case of electrical detection an

image slit is also used and this adds to the image size, i.e.

(2-15) $$W=Ms_0+s_i$$

where s_i is the image slit width.

It can also be shown that the resolution of the machine can be given by;

(2-16) $$R=Ms_0/D$$

(2-17) $$R=(Ms_0+s_i)/D$$

for photographic and electrical detection respectively. From these it can easily be shown that the uncertainty in a mass measurement, δ_m, is given by:

(2-18) $$\delta_m=fRm$$

where f is a constant factor for a given machine, ranging from 1/50 for a machine with photographic detection to 1/5000 for one with digitally aided electrical detection.

Fig. 2-1

Magnetic Sector

Fig. 2-2

Electrostatic Sector

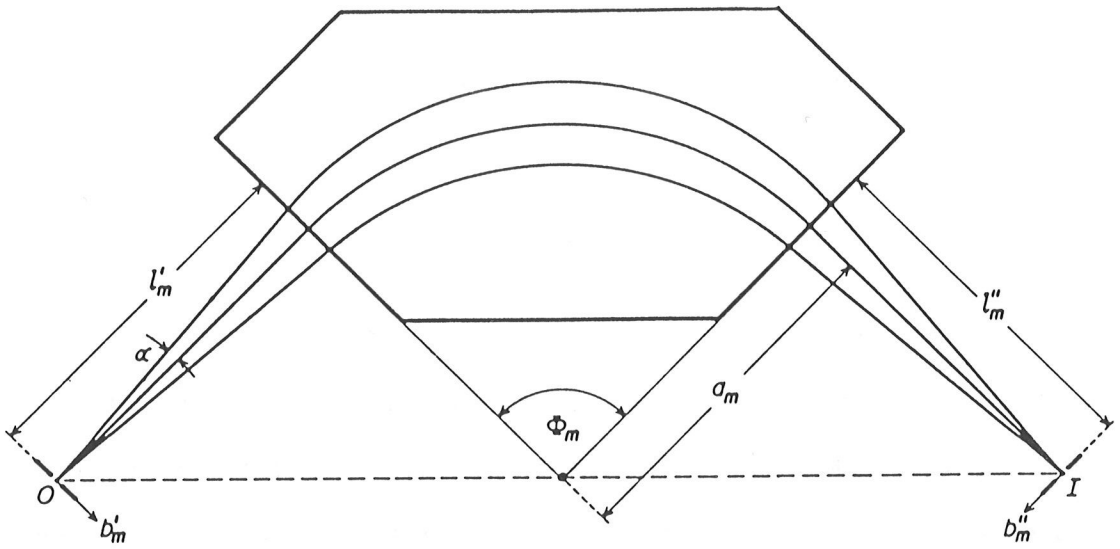
l'_m
α
Φ_m
a_m
l''_m
O
I
b'_m
b''_m

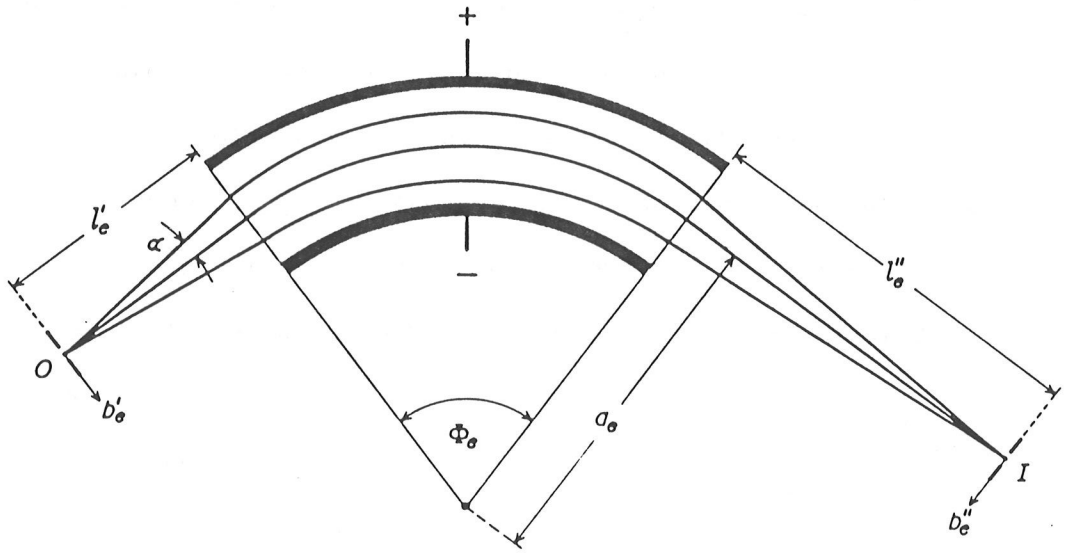
+
−
l'_e
α
Φ_e
a_e
l''_e
O
I
b'_e
b''_e

Chapter 3

The Manitoba 2

The research for this thesis was performed with the "Manitoba 2" high resolution mass spectrometer. The "Manitoba 2" is a second order double focusing machine designed in accordance with the theory of Hintenberger and Konig (1959). The overall geometry can be seen in Fig. 3-1 and block diagram can be seen in Fig. 3-2.

The machine can be divided into four major sections. These are the source region, the electrostatic analyser, the magnetic analyser and the collector region. Associated with each of these regions is supporting electronics including the "peak matching" electronics which will be considered along with the collector region. We will deal with each of these sections individually.

3.1 The Source Region

Included in this region is the source itself, the quadrupoles and steering plates, and the principal slit. The work herein was done using a "Finkelstein Source" (as described in Von Ardennes,

Fig. 3-1

Machine Geometry

a_e = 100·00 cm.
Φ_e = 94·65°
a_m = 62·74 cm.
Φ_m = 90°
l'_e = 44·45 cm.
l''_e = 17·63 cm.
l'_m = 82·49 cm.
l''_m = 59·46 cm.
ϵ' = 27°
ϵ'' = 15°
2k = 2·000 cm.

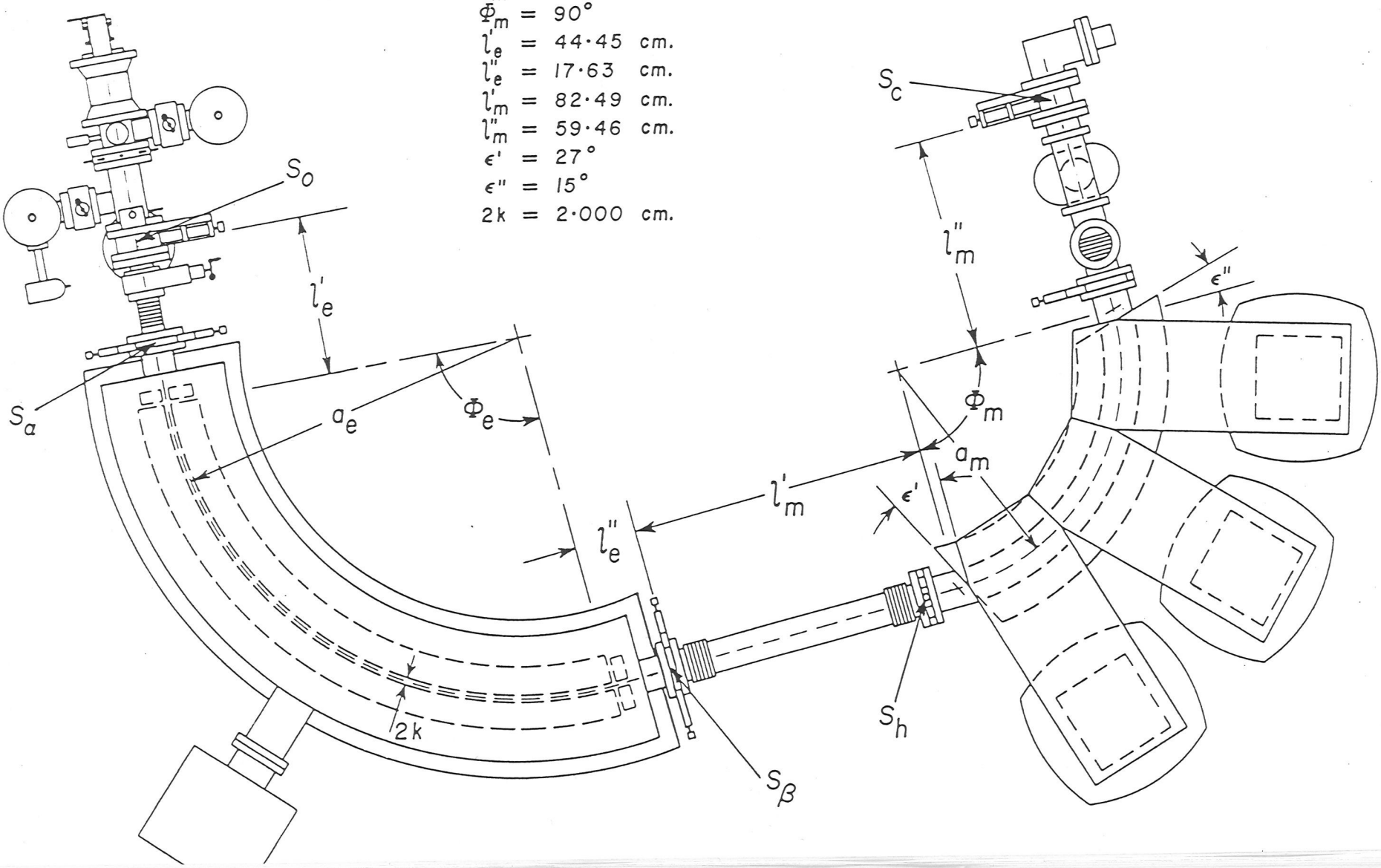

Fig. 3-2

Schematic Diagram of Manitoba 2

Including all Control Systems

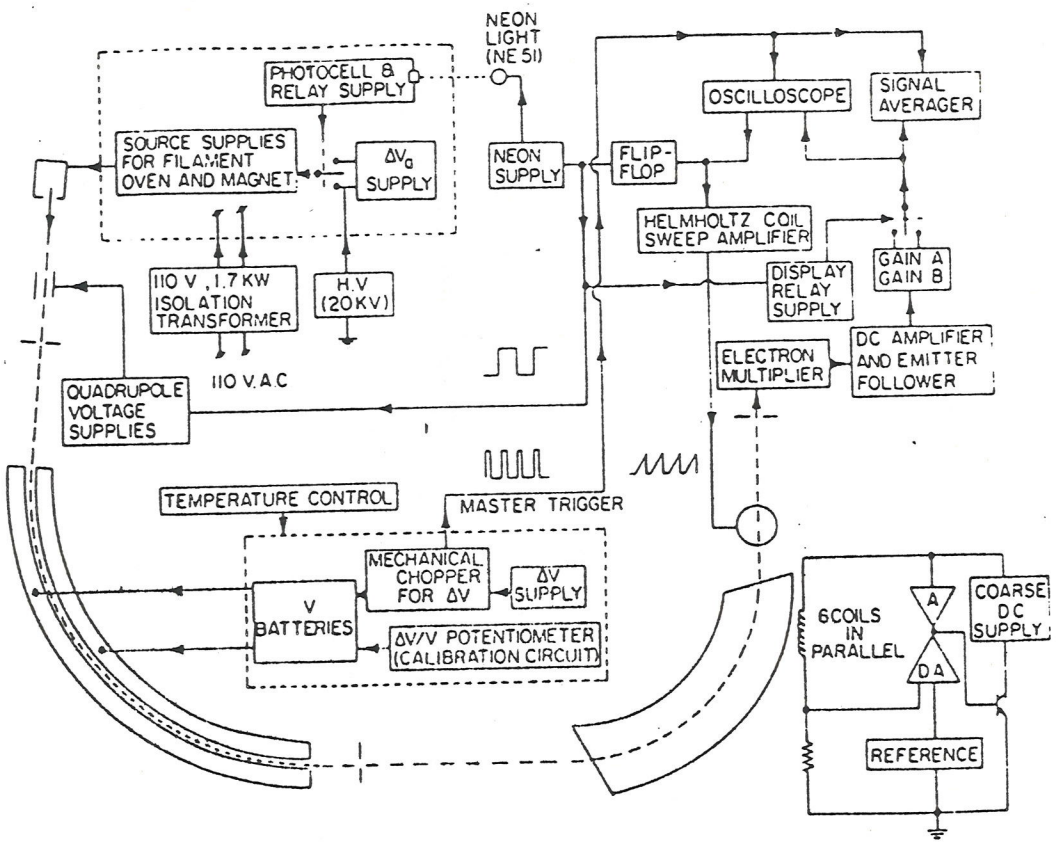
NEON LIGHT (NE 51)
PHOTOCELL & RELAY SUPPLY
SOURCE SUPPLIES FOR FILAMENT OVEN AND MAGNET
ΔV_a SUPPLY
NEON SUPPLY
FLIP-FLOP
OSCILLOSCOPE
SIGNAL AVERAGER
HELMHOLTZ COIL SWEEP AMPLIFIER
GAIN A
GAIN B
DISPLAY RELAY SUPPLY
110 V, 1.7 KW ISOLATION TRANSFORMER
H.V (20 KV)
110 V.A.C
QUADRUPOLE VOLTAGE SUPPLIES
ELECTRON MULTIPLIER
DC AMPLIFIER AND EMITTER FOLLOWER
TEMPERATURE CONTROL
MASTER TRIGGER
MECHANICAL CHOPPER FOR ΔV
ΔV SUPPLY
V BATTERIES
ΔV/V POTENTIOMETER (CALIBRATION CIRCUIT)
6 COILS IN PARALLEL
A
DA
COARSE DC SUPPLY
REFERENCE

Fig. 3-3

Source Arm of Manitoba 2

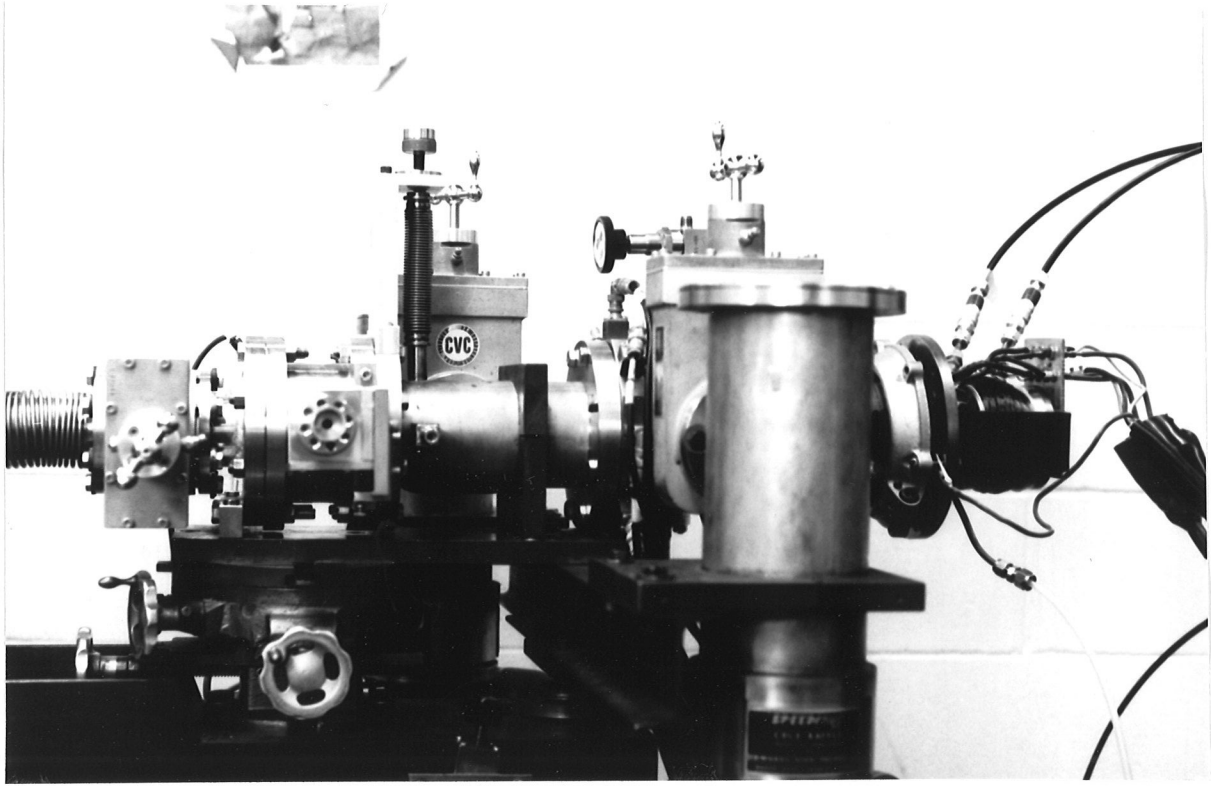
CVC

Fig. 3-4

Interior of the Source

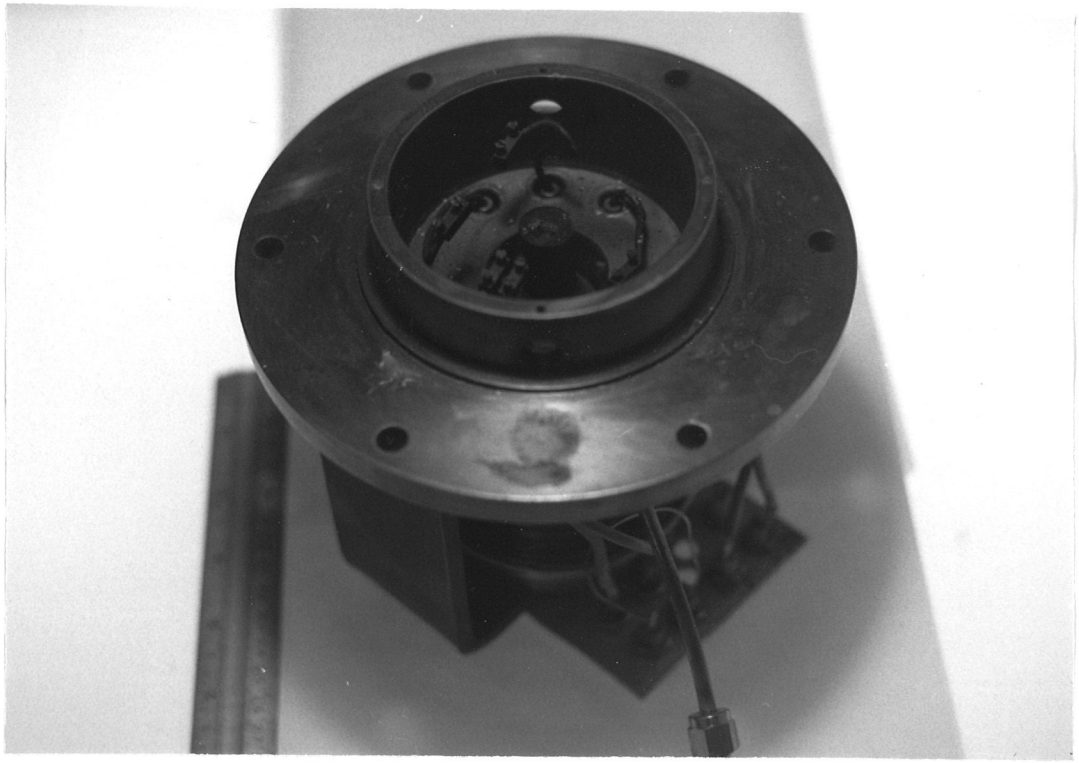

(1962)). The source parts, which are illustrated in Fig. 3-5, consist of: an oven, a steel cylinder approximately 4 cm by 1 cm with a 1 mm centred hole drilled transversly through it; a rhenium filament, centred beneath the oven; a repeller pole (also a pole for the axial magnetic field required for source operation) beneath the filament which, being negatively charged, repells electrons from the filament and through the oven hole; and a magnet coil providing an axial field which confines the electron beam to spiral trajectories.

The sample, which is either in gaseous or solid form, is leaked into or placed directly into the oven. It is in this region where ionization takes place, normally under plasma conditions. Because the source body is maintained at positive twenty thousand volts the positive ions are extracted from the hole at the front of the source.

After leaving the source the ions encounter first a pair of steering plates, which can move the beam either vertically or horizontally, and then a pair of electrostatic quadrupoles, forming a "quadrupole lens". This set up can be seen in fig. 3-6. The effect of the first quadrupole is to focus the ion beam in one plane, defocusing in the other, with the opposite being true for the second quadrupole (the two have opposite polarities). The net effect of the pair is focusing. After the beam illuminates the principal slit. As was noted in equation 2-17 , the resolving power is dependent upon the width of this slit. For

Fig. 3-5

Source and Approximate Potentials

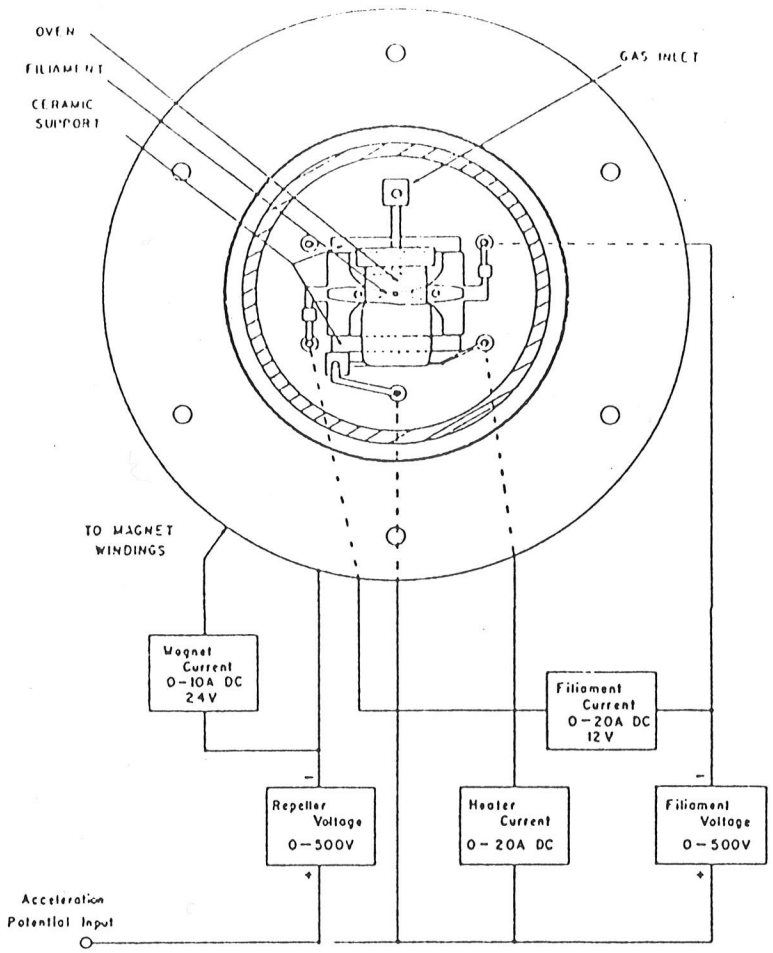

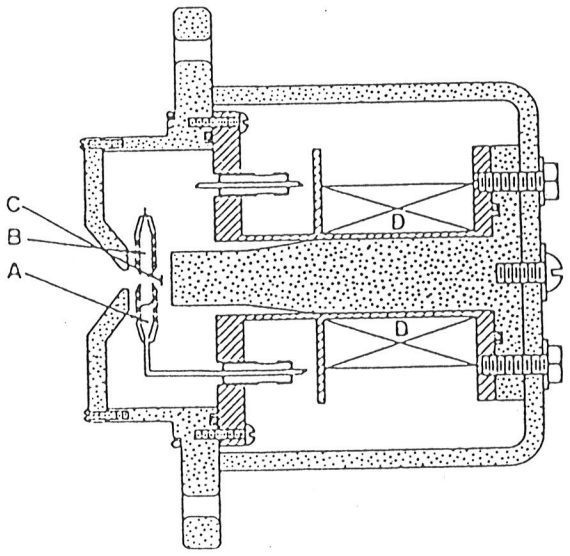

E

▨ BRASS

▦ IRON

A SAMPLE
B OVEN (stainless steel)
C Re FILAMENT

D Cu WINDINGS FOR $\vec{B}$

E 5 cm

Fig. 3-6

Quadrupoles and Steering Plates

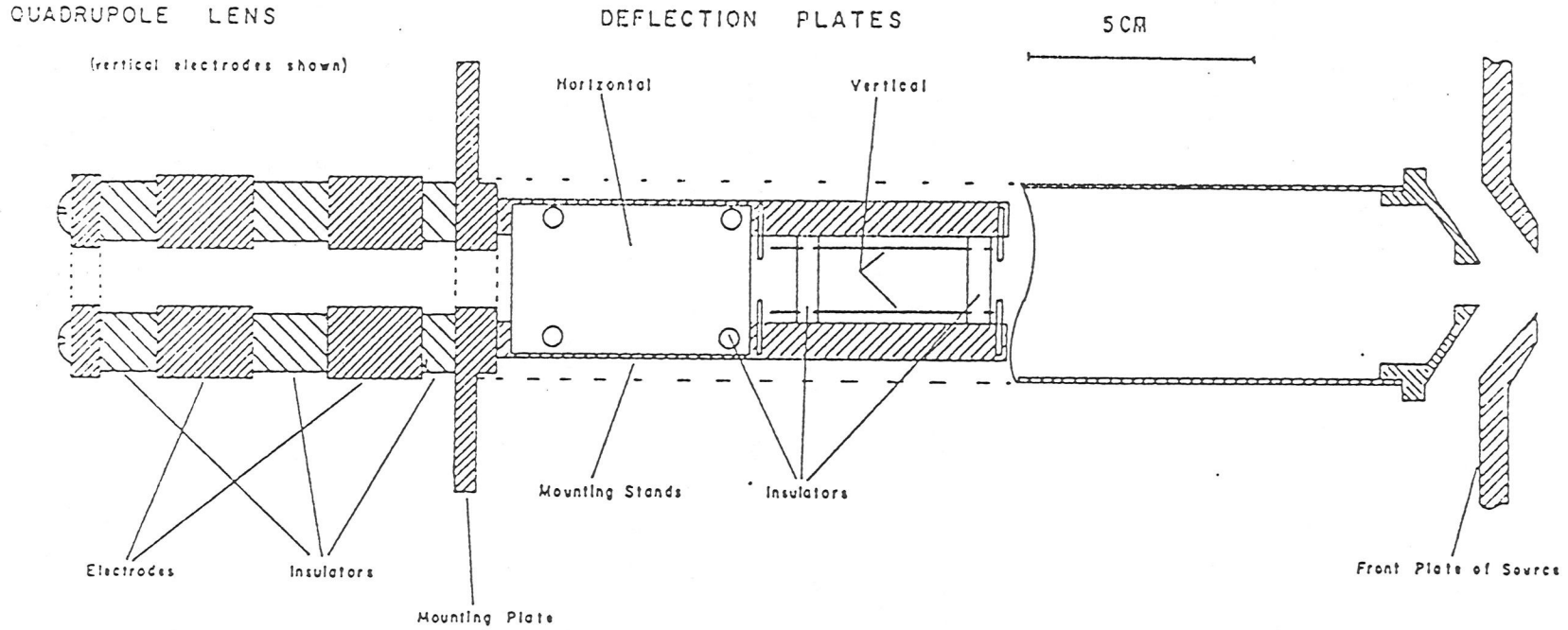

FOCUSSING AND STEERING ELETRODES

1/100,000 resolution the slit width should be approximately 5.4 micro-meters. A second slit, set at approximately 1.2 mm, and approximately 28 cm from the principal slit limits the beam spread (alpha) to 2×10^{-3} radians. The source region is mechanically mounted so that it can be moved in all three directions, with respect to the electrostatic analyser, to obtain adjustment.

3.2 The Electrostatic Analyser Region

After the ions have passed through these slits they enter the 1 m radius electrostatic analyser. This analyser consists of gold plated cylindrical electrodes, insulated with quartz blocks. The 2 cm gap between the two electrodes is maintained by quartz spacers. Batteries supply the plate voltage with the ends of the electrodes being terminated according to Herzog's theory (1935). This analyser is ball bearing mounted, set to pivot about its direction focus, with the analyser and the source region moving as one piece.

3.3 The Magnetic Analyser Region

Upon leaving the electrostatic analyser the energy spread of the beam is limited by a third slit (beta slit), this one having a width of 3 mm. The ions traverse a drift space, about 1 meter long, and then enter the magnetic analyser. The magnet yoke is in

Fig. 3-7

Electrostatic Analyser of Manitoba 2

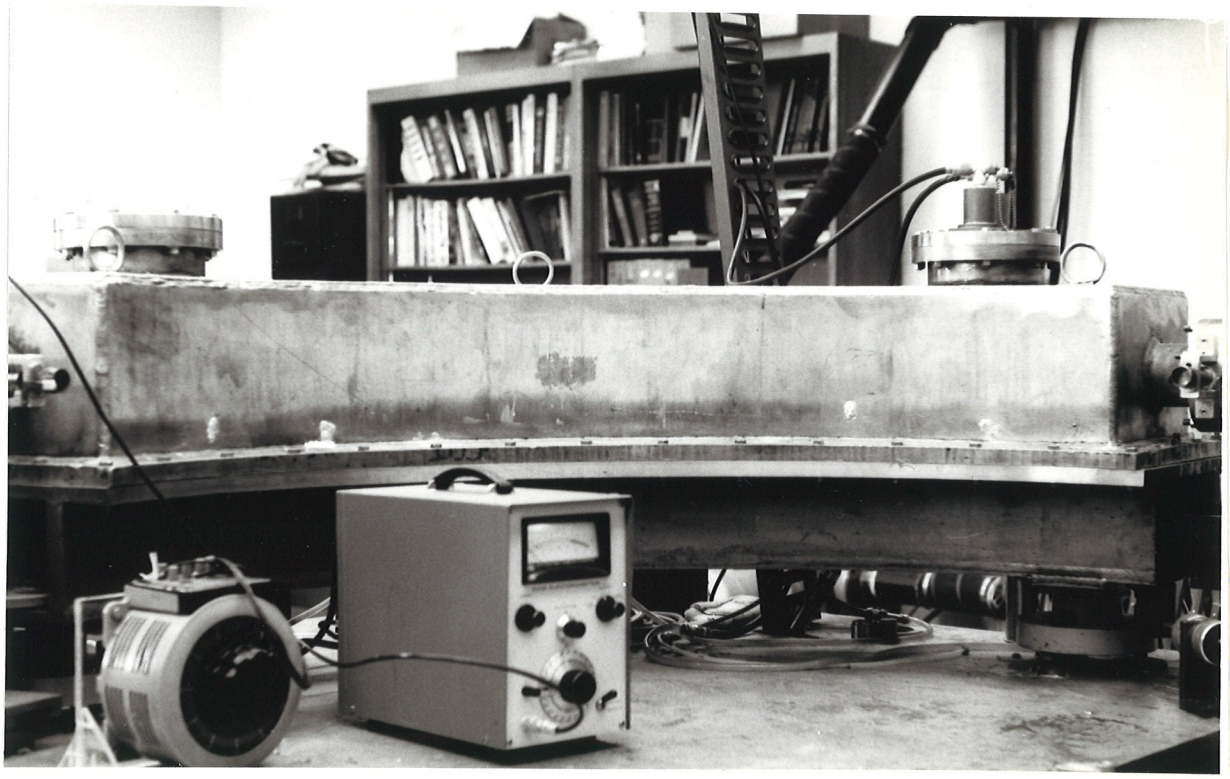

Fig. 3-8

Magnetic Analyser of Manitoba 2

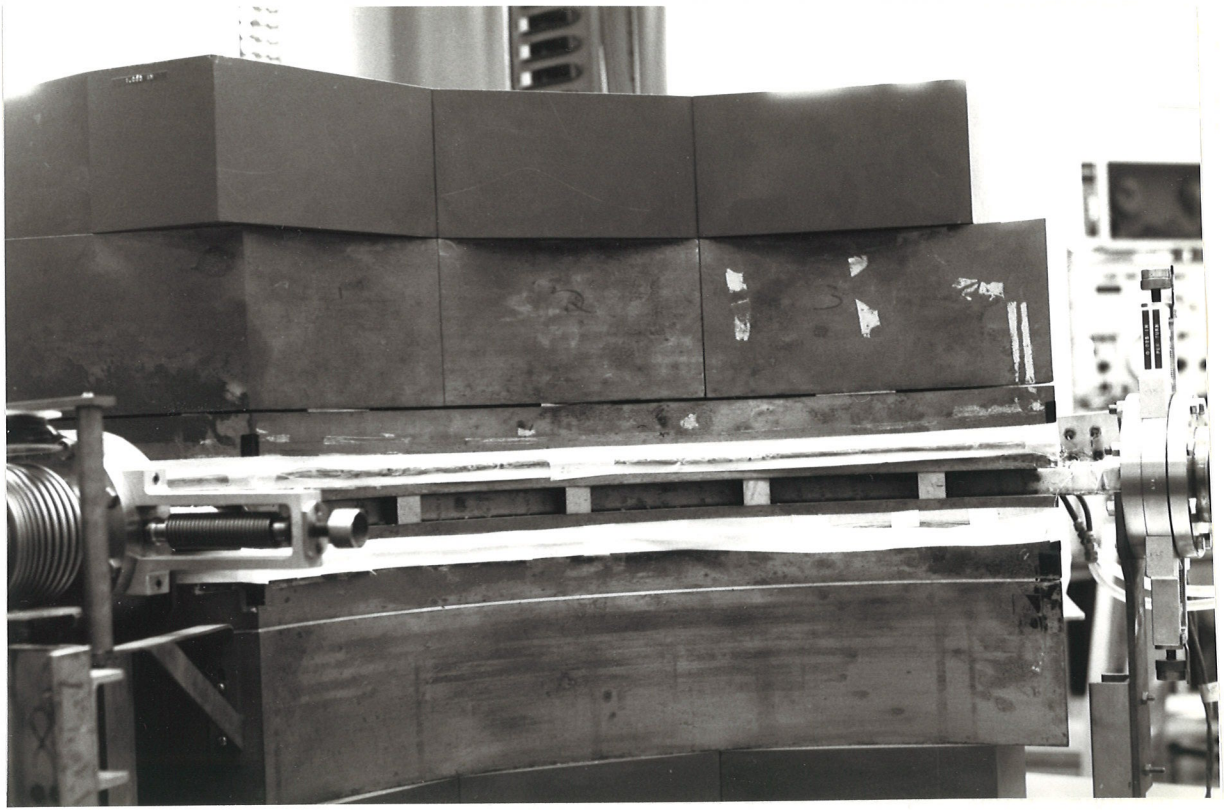

3 c-shaped sections, each with two coils. The pole face is machined from a single block of Armco iron, with a 2.5 cm gap. The magnet design also incorporates shimming gaps with aluminum spacers to smooth out irregularities in the field. Work done by Bishop (1969) indicates a field uniformity of 1/5000 at .3-.8 W/m^2 3 cm inside the physical boundary. The magnet supply stability circuitry can be seen in Fig. 3-9.

3.4 The Collector Region

After leaving the magnetic analyser the ions are swept across the collector slit by a Helmholtz pair, thereby pulsing the beam. The ions that pass through the collector slit are detected by a chaneltron electron multiplier. These pulses are fed into both to a "slow" amplifier, and then into a live display oscilloscope, and into a Nicolet signal averager. The signal averager displays the contents of it's memory, updated after each sweep, onto another oscilloscope.

Before closing this section a discussion of the machine's vacuum system is in order. In the source region a pressure of $1x10^{-6}$ torr to approximately $8x10^{-5}$ torr, depending upon the sample being ionized, is maintained by two 150 l/s diffusion pumps. Since the principal slit is very narrow quite a large pressure difference can be maintained between the source region and the rest of the machine. A pressure of $3x10^{-8}$ torr,

Fig. 3-9

Magnet Supply and Stability Circuitry

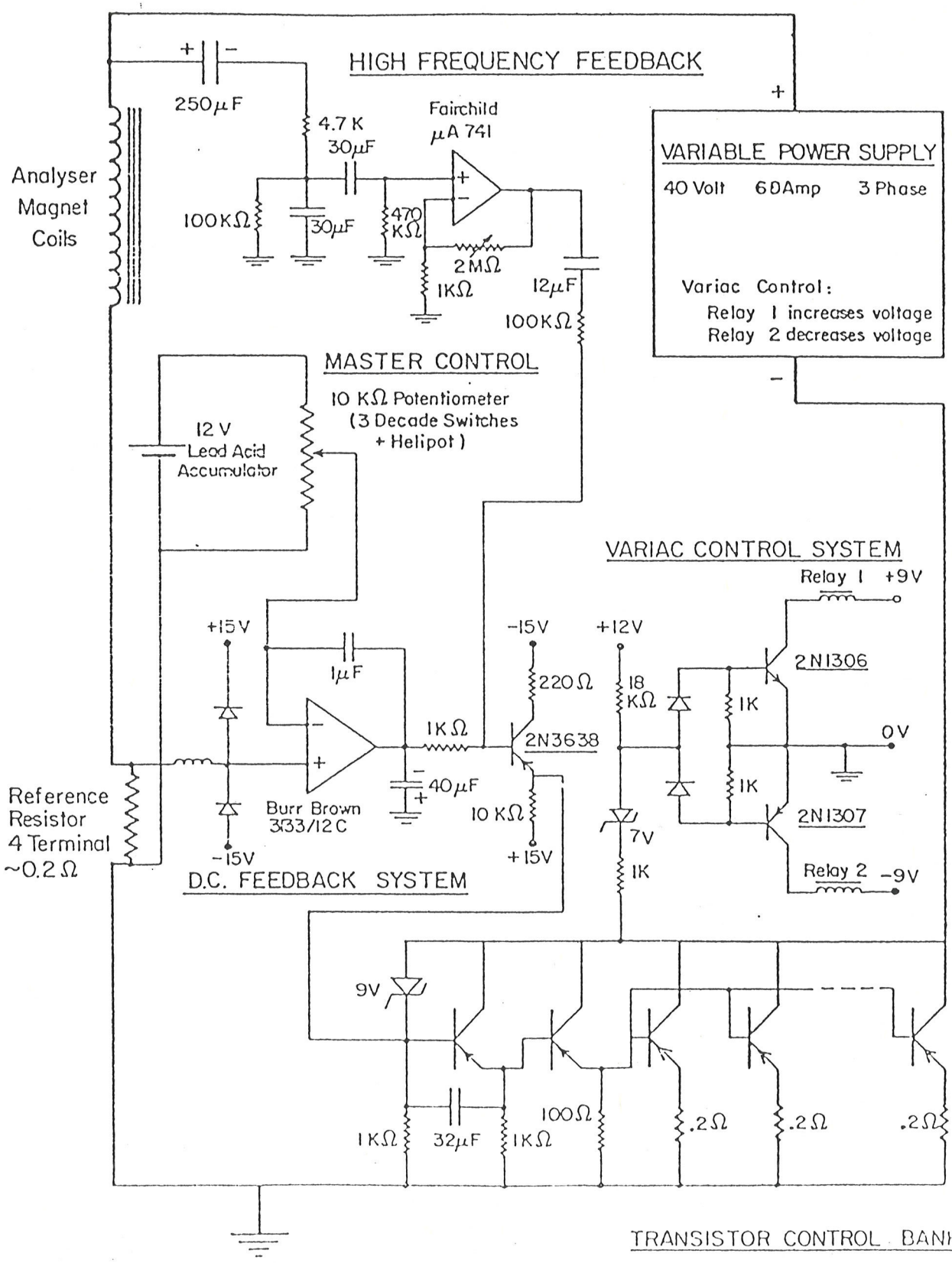
HIGH FREQUENCY FEEDBACK
250μF
4.7 K
30μF
Fairchild
μA 741
Analyser
Magnet
Coils
100KΩ
30μF
470
KΩ
2MΩ
1KΩ
12μF
100KΩ
VARIABLE POWER SUPPLY
40 Volt 60Amp 3 Phase
Variac Control:
Relay 1 increases voltage
Relay 2 decreases voltage
MASTER CONTROL
10 KΩ Potentiometer
(3 Decade Switches
+ Helipot)
12 V
Lead Acid
Accumulator
VARIAC CONTROL SYSTEM
Relay 1 +9V
+15V
1μF
-15V
+12V
220Ω
18
KΩ
2N1306
1K
1K Ω
2N3638
0V
1K
40μF
Reference
Resistor
4 Terminal
~0.2 Ω
Burr Brown
3333/12C
10 KΩ
2N1307
7V
-15V
+15V
1K
Relay 2 -9V
D.C. FEEDBACK SYSTEM
9V
1KΩ
32μF
1KΩ
100Ω
.2Ω
.2Ω
.2Ω
TRANSISTOR CONTROL BANK

Fig 3-10

Detector Arm of Manitoba 2

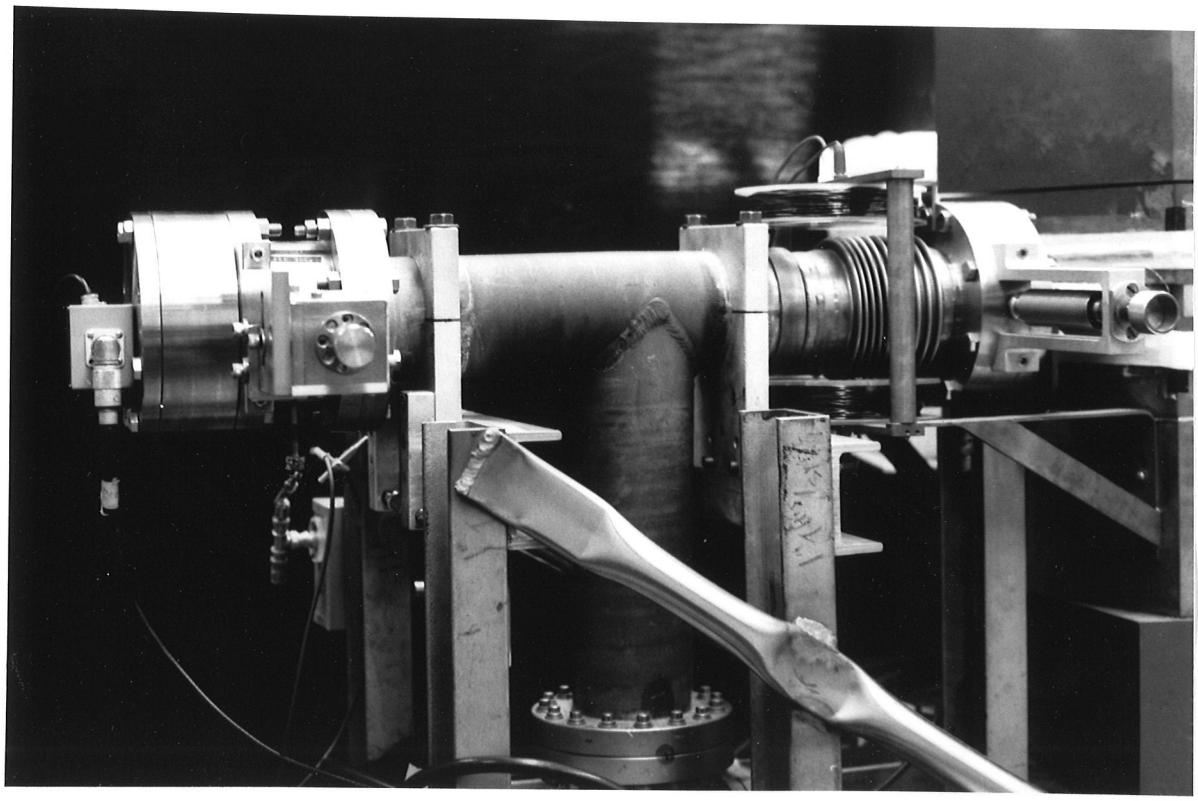

provided by a Leybold Turbotronik 150 1/s turbo pump at the mid way point of the electrostatic analyser and a 50 1/s ion pump at the collector end, is typical for the rest of the machine. The importance of low pressures after the principal slit can be seen by referring to equations 3-1 and 3-2. The mean free path is given by,

(3-1) $$\text{mean free path} = \lambda(\text{cm}) = 1/\sqrt{2}\, D^2 N = 0.005/P$$

where D is the molecular diameter, N the number of molecules per cubic centimeter and P the pressure in Torr. With the mean free path calculated, and given a path length X, one can calculate the number of unscattered particles, N, from an ion beam of N_0 particles, i.e.

(3-2) $$N = N_0 e^{-X/\lambda}$$

Thus, we note that as P increases λ decreases thereby causing an exponential growth in ion beam scattering. For Manitoba 2, operating at 3×10^{-8} Torr, λ=1666 m, and with X = 4.59 m we obtain a value of < .1% scattering. Ions that are scattered at small angles have the effect of contributing to the tails of the peaks.

Fig 3-11

The Manitoba 2


DANG
HIGH
VOLTAGE

Chapter 4

Experimental Details

This chapter includes a description of machine "run-up", measurement procedure and data analysis.

Machine "run-up" begins with the switching on of the source potentials (the approximate values can be seen in Fig. 3-2). Care is taken in setting the filament current, which is slowly increased to 10 A over a period of 5 min., to promote extended filament life. The maximum filament current is determined by limiting the emission current to 20 mA max. With the source pressure set to the desired value ($1x10^{-5}$ torr) by adjusting the input gas flow rate, the source high voltage is switched on. The other machine voltages and controls, including the quadrupoles, the Helmholtz coils, the detector, and electrostatic analyser voltage supply can be switched on either before or after the source potentials.

This all being completed, and with both slits opened wide and the sweep amplitude at a maximum, the main valve is opened allowing the ions into the machine. Vertical and horizontal steering plates are carefully adjusted until peaks appear on the

"live" oscilloscope screen.

The next step involves obtaining both direction and velocity focus, discussed previously in Chapter 2. Direction focus is checked by moving the beam from side to side with the horizontal deflective plate (giving the beam a path off the optic axis). Good direction focus is indicated by a peak which rises and falls, rather than moving right and left. Poor direction focus is corrected by adjusting l_e'. It should be noted that the best direction focus occurs at or near the "turn-around" which is found by moving the analyser about its pivot. When set up correctly a marked improvement in peak shape is seen at the turn-around. Next, the velocity focus is checked. A 10 V square wave is applied to the source on top of the normal high voltage. The square wave frequency is 1/2 of the sweep frequency, thereby allowing for simultaneous display of switched and unswitched peaks. These should appear one on top of the other, if there is a good velocity focus. If this is not the case the collector slit is moved radially in or out, increasing or decreasing the magnetic field to keep the peaks on the screen, until a velocity focus is obtained. It can be noted that once first order focusing is found, second order focusing is assured (Barber, 1965). Thus no additional changes are necessary to get second-order focusing.

4.1 Peak Matching

Once the desired doublet is obtained and direction and velocity focusing have been realized, the work then proceeds to measuring the mass difference between the pair. If one of the members is one of or a combination of ^{12}C, ^{13}C, ^{35}Cl, ^{37}Cl, ^{16}O or ^{1}H then an absolute mass measurement is being made of the second member. Otherwise it is a relative mass difference that is being measured.

The two peaks, corresponding to the two differing masses, are produced by ions traversing slightly different paths between source and collector, the "heavier" group being to the outside and the "lighter" group to the inside within the magnetic analyser. By Bleakney's Theorem (Bleakney, 1936; Swann, 1931) the two ion groups of masses m and m' can be made to follow identical paths in the electro-magnetic fields if all electric fields are switched proportional to the mass difference, i.e.

$$\frac{m}{m'} = \frac{V'}{V} \tag{4-1}$$

Thus, square waves of previously calculated voltages are applied to the accelerating voltage, the quadrupoles, the deflection plates and the electrostatic analyser plates. As a result of the chosen geometry the switched voltages applied to the source, the quadrupoles and the steering plates need only be accurate to about 1%, these having only a small effect on the ion path. The voltage applied to the electrostatic analyser has the

greatest effect on the ions and produces a lateral displacement. It is therefore measured very accurately, to a precision of (1 / $2x10^{-9}$)V by means of a Julie Research voltage divider as part of a null circuit. All of the above voltages are switched at one half the sweep frequency and thus, when all voltages are correctly set up, the two peaks will be superimposed.

4.2 Visual Null Matching

The following method is used to determine when the two peaks are superimposed. An estimated m is used to determine the switching voltages. Alternate sweeps are fed through different amplifiers, A and B, giving a dual trace (see Fig. 4-1) with one member of the doublet appearing above the other. The gains of the two amplifiers can be adjusted so that the two have equal amplitude. These two signals are fed into a Nicolet signal averager with one being added and the other subtracted from the signal averager memory. If the two are not matched an S-shaped signal is observed (Fig. 4-2a). If they are matched an oval-shaped signal noise results (fig. 4-2b). This condition is obtained by varying V_e (the voltage on the Electrostatic analyser), and this voltage is measured once the desired signal is set up. In order to account for possible systematic effect, the following conditions are altered, giving 8 different combinations which constitute a single run:

Fig. 4-1

Live Display; Switched and Unswitched Peaks

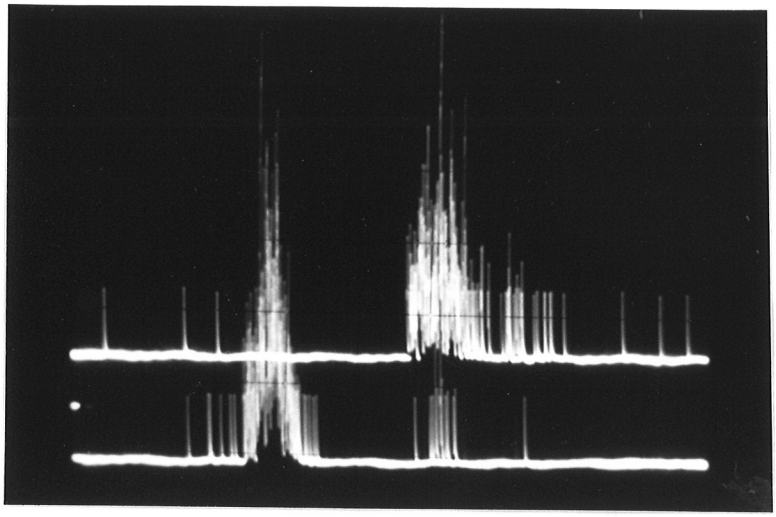

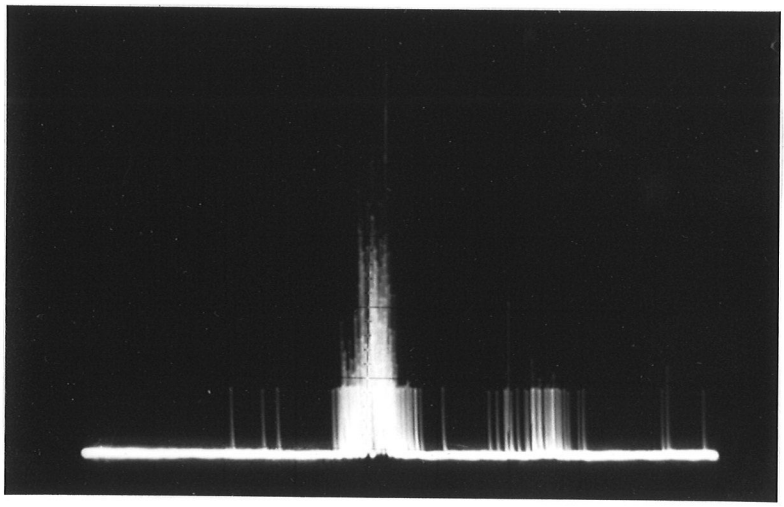

Fig. 4-2a

Unmatched Peaks

Fig. 4-2b

Matched Peaks

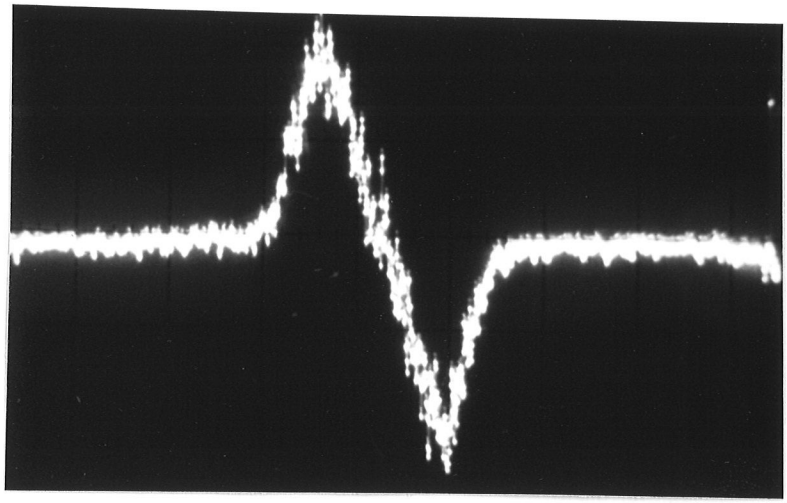

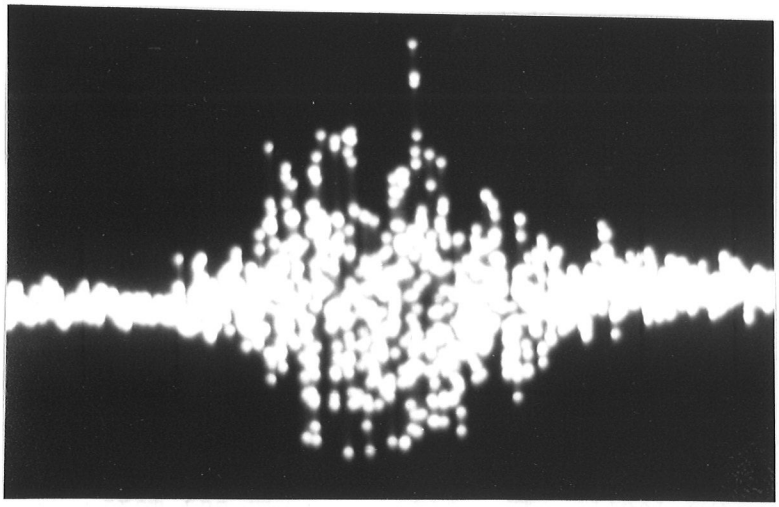

a) sweep direction is set forward, or reverse

b) V_e polarity is changed (add or subtract)

c) amplifiers A and B are exchanged

The eight different values obtained are averaged thus giving a result m m.

The presence of unswitched voltages, e.g. localized charging on the analyzer plates, can cause systematic effects. This is corrected for by measuring a calibration doublet, usually one member of the measure doublet matched to a peak one or two mass numbers away. A resulting correction can then be applied to the doublet being measured. This correction is made by adding the error in parts per million to the measured value, where the error in parts per million is given by,

$$Eppm = [m(theoretical) - m(measured)]/ m(measured)$$

4.3 Computer Matching:

Computer matching involves storing information on the doublet in question on computer tape and then having this analysed by computer at a later time. The method of obtaining this information differs from the visual method. The signal averager is used in pulse counting mode and collects four different signals. On one of the four sweeps V_e is applied to the plates

with smaller voltages V_1 and V_2 ($V_1 = -V_2$) being applied on two other sweeps and finally 0 volts is applied to the fourth (see Fig. 4-3). The four signals are accumulated in different quadrants of the signal averager. The result of the above procedure is to 'bracket' the matched condition, i.e. set up an upper and lower bound to the correct match voltage, and a centroid peak matching routine is performed by the computer.

Again, in order to eliminate systematic errors a single run consists of eight measurements by varying the following parameters:

1) Forward or reverse sweep
2) Add or subtract V_e -
3) Change polarity of the V_1 and V_2

Computer matching has the advantage of being more precise, with one computer run being equivalent to approximately 6 visual runs. Also, fluctuations in peak intensity are not a problem, however the peaks must not shift laterally during the measurement.

4.4 Timing

Timing is thoroughly discussed in previous theses (see Sharma 1979). The timing signals for both visual and computer matching are provided by Guildline choppers. The output square waves from these choppers turn on and off the appropriate voltages in

Fig. 4-3

Schematic of Computer Match

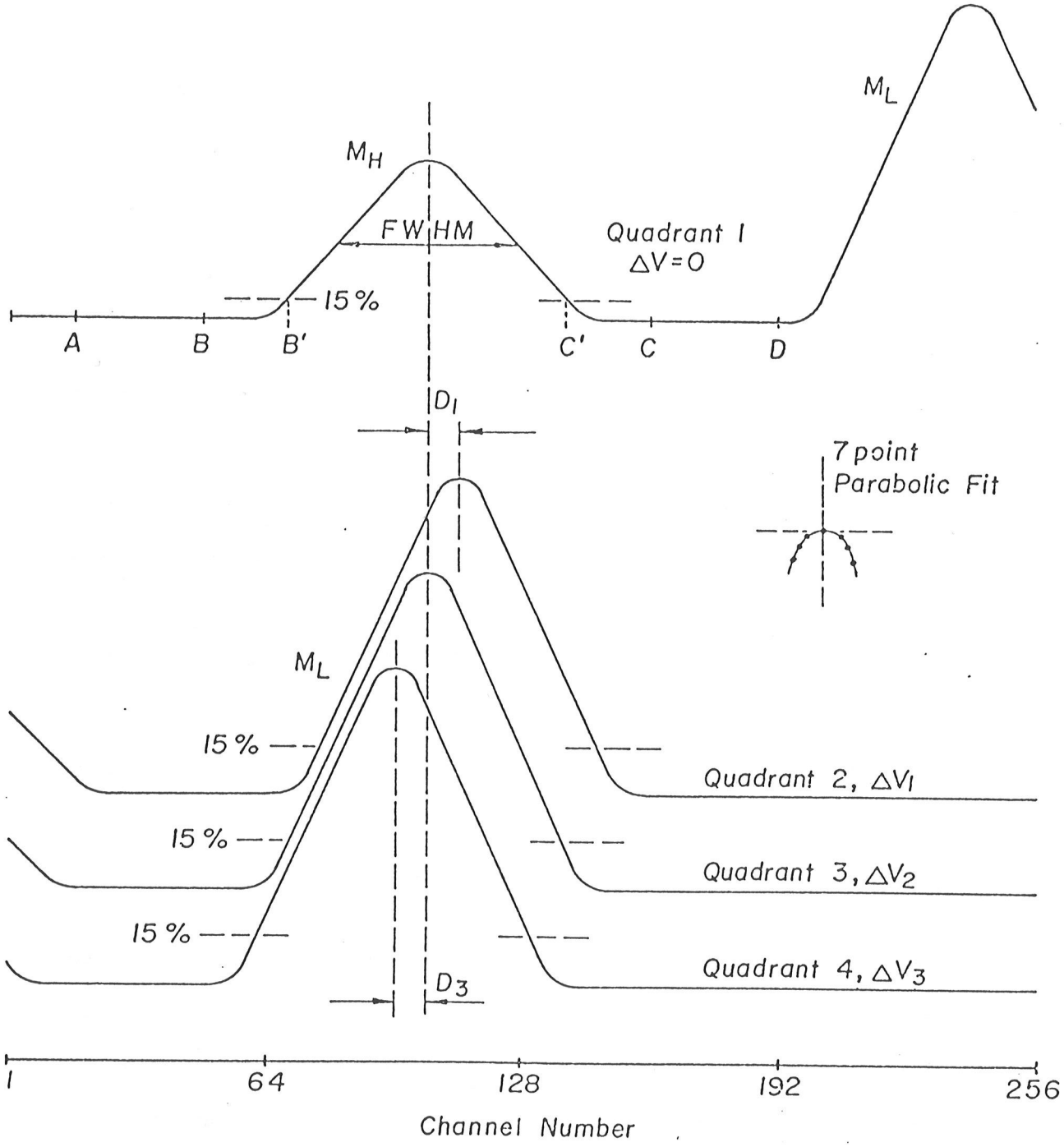
M_L
M_H
FWHM
Quadrant I
$\Delta V = 0$
15 %
A
B
B'
C'
C
D
D_1
7 point
Parabolic Fit
M_L
15 %
Quadrant 2, ΔV_1
15 %
Quadrant 3, ΔV_2
15 %
Quadrant 4, ΔV_3
D_3
1
64
128
192
256
Channel Number

sequence and can be seen schematically in Figs. 4-4 and 4-5.

4.5 Data Analysis:

A final result for any given doublet is obtained by calculating the weighted mean, i.e.

$$(4\text{-}2) \qquad Xwm = \left(\sum_i x_i/\sigma_i^2\right) / \left(\sum_i 1/\sigma_i^2\right)$$

with an error being given by the larger of the internal or external error, i.e.

$$(4\text{-}3) \qquad \sigma_{int}^2 = 1/\left(\sum_i 1/\sigma_i^2\right)$$

$$(4\text{-}4) \qquad \sigma_{ext}^2 = \left(\sum_i (Xwm-x_i)^2/\sigma_i^2\right) / \left(\sum_i 1/\sigma_i^2\right)(N-1)$$

The number of runs needed to complete a measurement can vary from ten to forty, depending upon the difficulty of measurement, e.g. low intensity of one or both members of the doublet, the self consistency of the measurements, how fast the error is coming down. Errors in the neighbourhood of 1 keV at mass 100 are routine.

Fig. 4-4

Timing for Visual Match

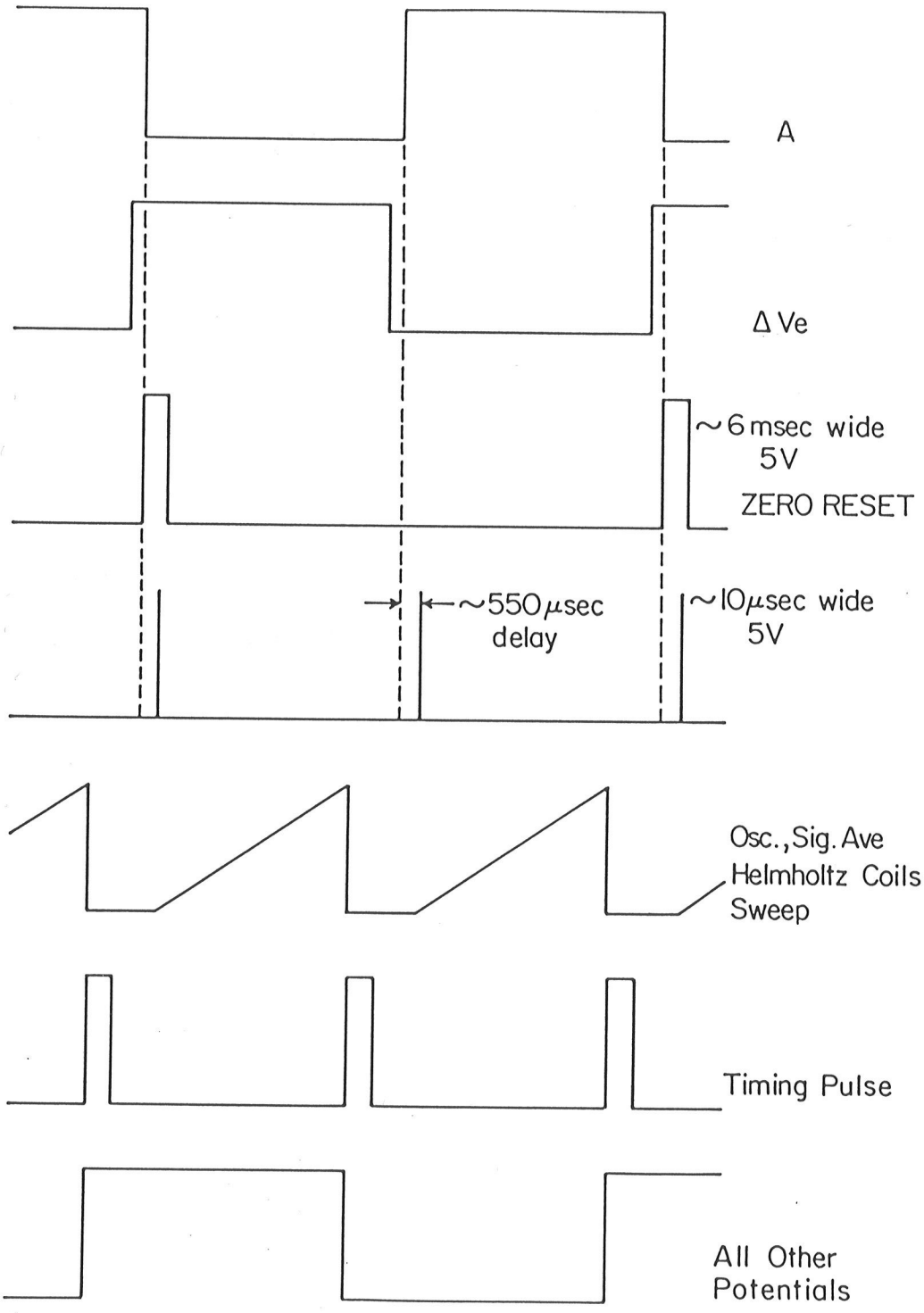
A
Δ Ve
~6 msec wide
5V
ZERO RESET
~550μsec
delay
~10μsec wide
5V
Osc., Sig. Ave
Helmholtz Coils
Sweep
Timing Pulse
All Other
Potentials

Fig. 4-5

Timing for Computer Match

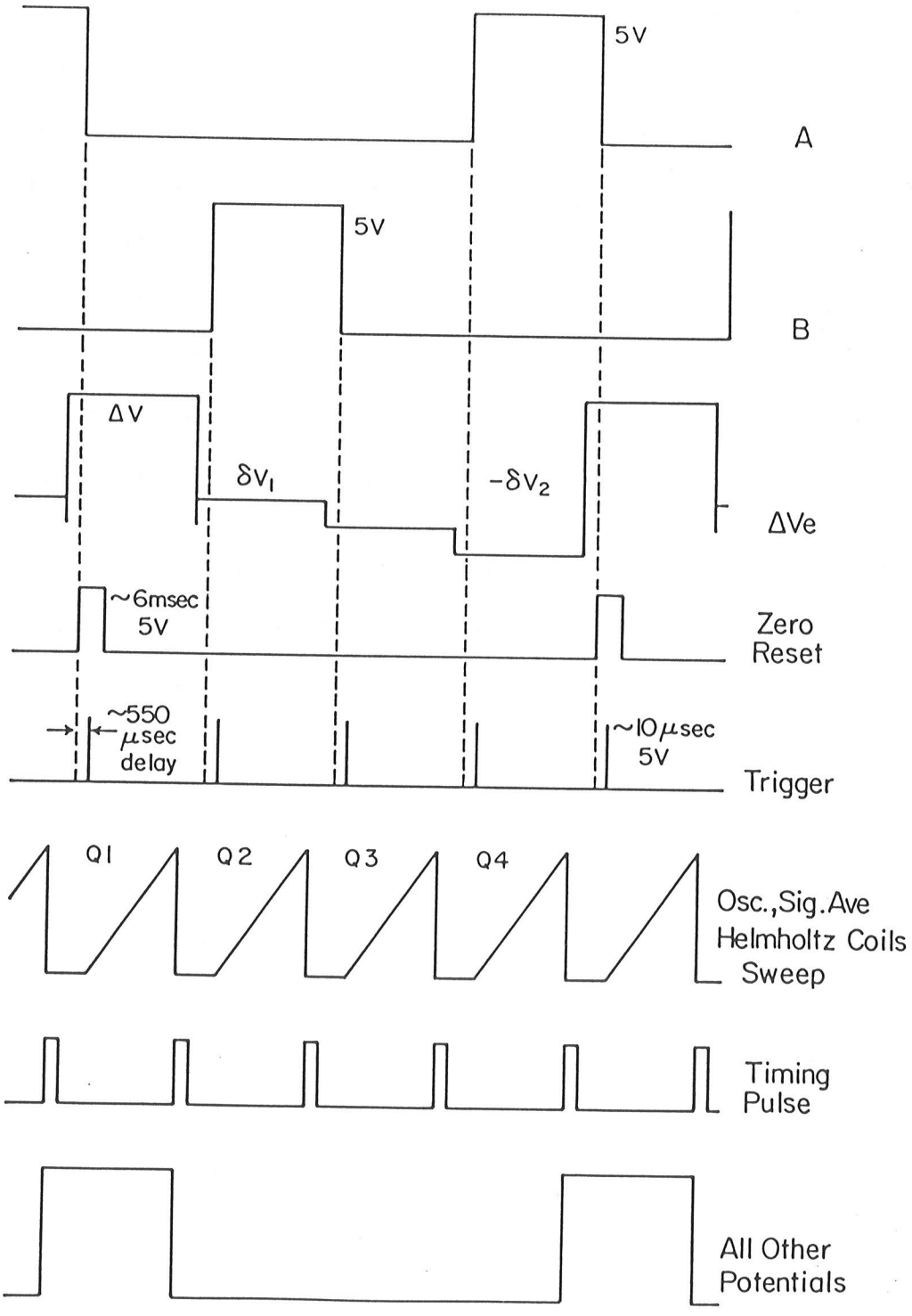
5V
A
5V
B
ΔV
δV1
-δV2
ΔVe
~6msec
5V
Zero
Reset
~550
μsec
delay
~10μsec
5V
Trigger
Q1
Q2
Q3
Q4
Osc., Sig. Ave
Helmholtz Coils
Sweep
Timing
Pulse
All Other
Potentials

Most often one is able to make several measurements of different doublets at the same mass number or one mass number apart. This allows "mass loops" to be formed, e.g. if the masses a, b and c are measured as follows; a - b, b - c, a - c, then the value given by the equation (a - b) + (b - c) - (a - c) should be near zero and less than the square root of the sum of the squares of the individual doublet errors. If several loops are formed the componenet masses become overdetermined and "best" values may be calculated by a least squares evaluation.

With the least squares adjustment performed (Ellis, 1983) a check of the consistancy of the data is performed. This is done by looking at the reduced chi-squared or Birge ratio values (Birge, 1932).

The relevant equations are the following. The reduced chi-squared is formed by evaluating the chi-squared for the data and then dividing by the number of degrees of freedom, i.e.

$$\chi^2 = \Sigma(r_i/\sigma_i)^2 \qquad (4\text{-}5)$$

The Birge ratio is given by:

$$(\chi^2/F)^{1/2} \qquad (4\text{-}6)$$

where r_i is the residual, or the difference between input and output values of the least squares adjustment, σ_i is the input

error and F is the number of degrees of freedom.

The value for the reduced chi-squared should be near one. The value for the Birge ratio should fall between theoretically calculatable limits given by J. Mattauch (1960). These limits are calculated as follows,

$$(\chi^2/F)^{1/2} = 1 \pm (1/2F)^{1/2} \qquad (4\text{-}7)$$

Chapter 5

Results

In particular, this thesis is based upon precise atomic mass determinations at A = 124. Relative atomic mass measurements were made among ^{124}Xe, ^{124}Te, ^{124}Sn and $^{54}Fe^{35}Cl_2$, with absolute atomic mass measurements being made between these and $^{13}C^{37}Cl_3$ (A = 124). Also, a method of systematic corrections, first adopted by R. L. Bishop in 1969, was employed. Calibration doublets used were ^{124}Te - ^{122}Te, ^{125}Te - ^{124}Te and $^{12}C^{37}Cl_3$ - $^{13}C^{37}Cl_3$ with corrections of 180 ppm being routine although they did range as high as 350 ppm.

It should be noted at this point that the impetus for these measurements came from the systematic approach this lab is making towards the determination of double beta decay energies, a subject which has regained prominence in recent years. This resurgence is due in part to the possibility of using double beta decay experiments to determine the mass of the neutrino. It should also be noted that the error attached to the value for ^{124}Xe (123.90612 +150) in the 1977 atomic mass evaluation of Wapstra and Bos,and is attributed to R. E. Halsted, is unusually high, the largest by far for any naturally-occurring nuclide, and is

considerably reduced in this work.

Eight doublet spacings were determined to have the values presented in Table 5-1. With these eight doublets five loops can be formed (see Table 5-2). This allows a least squares adjustment to be performed on the data. Results of this adjustment are given in Tables 5-3 and 5-4 along with the difference between the "new" value and that given in the 1977 atomic mass evaluation of Wapstra and Bos. Most striking is the shift of 227 u for ^{124}Xe, this being greater than the error given in the 1977 mass table. From private communications with Wapstra we find that the new number for ^{124}Xe herein presented is in good agreement with recent decay experiments in this region.

Also of note is the $^{124}Xe - {}^{54}Fe^{35}Cl_2$ doublet. This links two masses over a relatively large section of the mass table and should have a significant effect as a constraint upon further least square evaluations. In this respect it should play the same role as the wide rare earth chloride doublets reported by Southon et.al. (1977) and used in the 1977 Mass Evaluation (Wapstra and Bos, 1977).

Table 5-1

Raw Data

FINAL DOUBLET VALUES (μ mass units)

#	DOUBLET	VALUE
1)	$^{124}Xe-^{13}C^{37}Cl_3$	4831.15 $\pm$ 1.78
2)	$^{124}Xe-^{54}Fe^{35}Cl_2$	28575.81 $\pm$ 0.99
3)	$^{124}Xe-^{124}Te$	3076.00 $\pm$ 1.78
4)	$^{124}Sn-^{13}C^{37}Cl_3$	4210.47 $\pm$ 0.76
5)	$^{124}Sn-^{124}Te$	2458.51 $\pm$ 0.89
6)	$^{124}Te-^{13}C^{37}Cl_3$	1754.63 $\pm$ 1.26
7)	$^{124}Te-^{54}Fe^{35}Cl_2$	25499.46 $\pm$ 2.74
8)	$^{13}C^{37}Cl_3-^{54}Fe^{35}Cl_2$	23744.46 $\pm$ 1.26

Table 5-2

Loop Closures

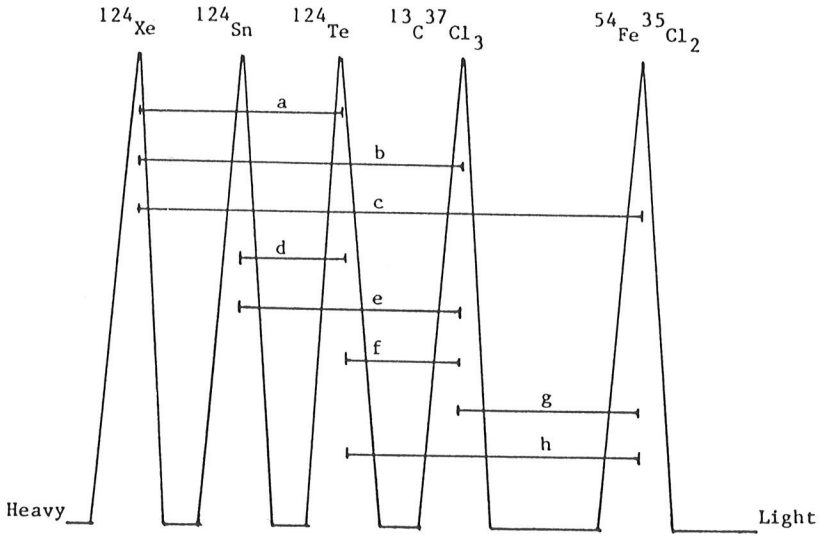

a + b - c

a + f - b

d + f - e

f + g - h

g + b - c

Table 5-3

Adjusted Values

	DOUBLET	INPUT VALUES	OUTPUT VALUES	OUT-IN	CHISQ
1)	^{124}Xe (ABS)	123905894.80 + 1.58	123905894.18 + 0.97	-0.62	0.1540
2)	$^{124}Xe-^{54}Fe^{35}Cl_2$	28575.78 + 0.99	28575.78 + 0.85	-0.02	0.0005
3)	$^{124}Xe-^{124}Te$	3076.00 + 1.78	3076.86 + 1.05	+0.86	0.2329
4)	^{124}Sn (ABS)	123905274.14 + 0.71	123905274.80 + 0.63	+0.66	0.8579
5)	$^{124}Sn-^{124}Te$	2458.51 + 0.89	2457.48 + 0.72	-1.03	1.3480
6)	^{124}Te (ABS)	123902818.30 + 1.26	123902817.32 + 0.76	-0.98	0.6038
7)	$^{124}Te-^{54}Fe^{35}Cl_2$	25501.65 + 2.56	25498.92 + 1.06	-2.73	1.1383
8)	$^{54}Fe^{35}Cl_2$ (ABS)	123877319.10 + 1.26	123877318.40 + 0.94	-0.70	0.3067

where (ABS) indicates that carbon and chlorine masses have been subtracted. All values in micro mass units.

Table 5-4

Final Values; Comparison with 1977 Mass Table

	NUCLIDE	ADJUSTED MASS	NEW VALUE - 1977 MASS EVALUATION
1)	^{124}Xe	123905894.18 + 0.97	-225.9 + 150.
2)	^{124}Te	123902817.32 + 0.76	-7.7 + 4.1
3)	^{124}Sn	123905274.80 + 0.63	+3.8 + 5.0
4)	$^{54}Fe^{35}Cl_2$	123877318.40 + 0.94	+0.9 + 1.8

All values in micro mass units.

Table 5-5

Error Analysis

For the doublets listed in Table 5-3 the following error analysis is obtained.

Number of Degrees of Freedom = 4

Sum of all Chi-Squared contributions = 4.64

Reduced Chi-Squared = 1.16

Birge Ratio = 1.08

| Theoretical Birge Ratio should be in the range 0.65 to 1.35 |

The birge ratio is within the given range indicating that the data is consistent.

The value for the reduced chi-squared which is slightly greater than 1 indicates small systematic effects.

5.1 Double Beta Decay

As was noted in an earlier chapter,atomic mass measurements can be extremly important data for nuclear physics. Looking at Fig. 5-1 we can see that along the line of constant A the stable isotopes are separated by Z = 2 between ^{124}Te and ^{124}Sn. This suggests the possibility of double beta decay from ^{124}Sn to ^{124}Te. Double beta decay is a process whereby nuclei with long half lives decay, along a line of constant A (i.e. A,Z ----> A,Z+2), by emitting two electrons, either positive or negative. This emission is accompanied by the production of two neutrinos or two anti-neutrinos. In an experimental search for double beta decay the mass difference between parent and daughter is of great importance. This can be seen by refering to equation 5-1;

(5-1) $$ {}^{A}X_{Z} - {}^{A}Y_{Z+2} = 2\beta^{\pm} + Q_{2\beta^{\pm}} $$

where $Q_{2\beta^{\pm}}$ is the sum of the kinetic energies. If the mass of the neutrino is zero then Q is the mass difference. A precise value for this energy can be determined by mass spectrometric methods thus allowing experimenters to set reasonably narrow energy windows when searching for this beta emission. This is quite important since the decay rate is extremely small and noise becomes a major difficulty.

Fig. 5-1

Section of Chart of the Nuclides

Showing Region of A=124 -

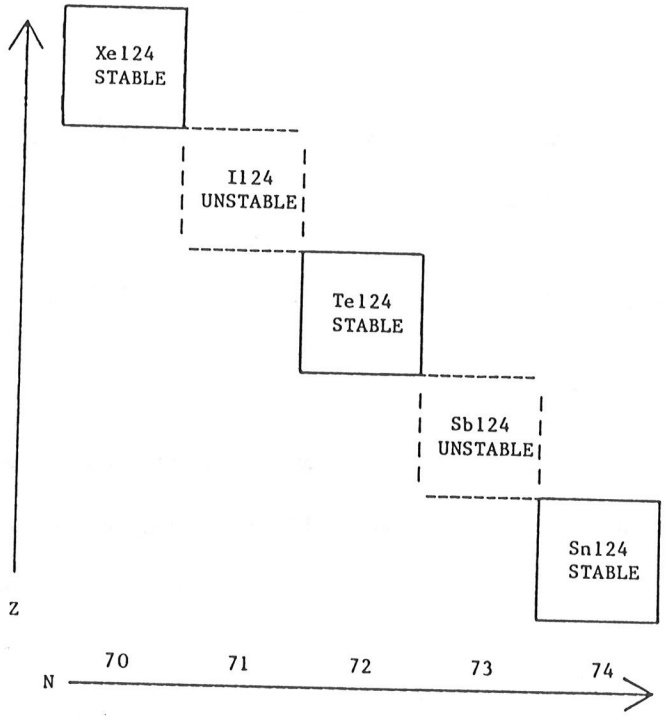
Xe124
STABLE
I124
UNSTABLE
Te124
STABLE
Sb124
UNSTABLE
Sn124
STABLE
Z
N
70
71
72
73
74

In this work I am able to present two double beta decay energies which are a significant improvement over the values obtained via the 1977 Atomic Mass Evaluation. These are:

(1) $^{124}Xe-^{124}Te = 2865.30 \pm 1.66$ keV (new value)

cf.: $^{124}Xe-^{124}Te = 3069.3 \pm 139.8$ keV (1977 mass table)

(3) $^{124}Sn-^{124}Te = 2290.11 \pm 0.83$ keV (new value)

cf.: $^{124}Sn-^{124}Te = 2278.45 \pm 5.96$ keV (1977 mass table)

One can see a significant improvement in the new values, an improvement which might considerably aid an experimenter in a search for double beta decays.

5.2 The Atomic Mass Table

Frequent mention is made throughout this thesis of the Atomic Mass Evaluation carried out by Wapstra et al (1971, 1977). This thesis would not be complete without a more detailed discussion of this mass evaluation.

Mass data is collected from both reaction and mass spectrometric methods. Thus, over the years, a large body of mass data has become available. This includes 3829 nuclear reaction energies and 1197 mass doublets as of 1977, on 1988 atomic masses (Wapstra et al, 1977). For various reasons, discussed thoroughly by Wapstra (1977), a number of these data are disregarded. The remaining data are subject to a least squares adjustment involving 1787 equations in 702 unknowns.

An interesting feature of this evaluation is the existence of a "backbone" of well known values along the line of beta-stability. Most of the links along this backbone are between values of A= 0, 1, 2 and 4. Thus, the precision of relative atomic masses decreases somewhat in regions removed from the absolute mass measurements, with the least squares adjustment having to pull these values into line.

As was mentioned earlier, a significant contribution is made in this work by measuring the absolute masses of ^{124}Xe and ^{54}Fe and the mass difference between the two. The effect of knowing these masses and this mass difference, to errors on the order of 1 keV, is to anchor the mass table at two points 70 mass units apart and set a constraint on the sum of many mass differences between these points. This in turn will affect future least squares adjustments.

Table 5-6

Auxiliary Data

This table contains data used extensively throughout this thesis. Mass values are from The 1977 Atomic Mass Evaluation (Wapstra and Bos).

Frequently Used Masses (micro mass units)

^{13}C	13003354.839 + 0.017
^{35}Cl	34968852.729 + 0.068
^{37}Cl	36965902.624 + 0.105

Energy to Mass Conversion

1 MeV = 1073535.5 + 3.0 nu

References

Austin, W. E., Holme, A. E. & Leck, J. H. (1976). Quadrupole Mass Spectrometry and its Applications, ed. P. H. Dawson. Amsterdam, Oxford, New York: Elsevier.

Bainbridge, K. T. (1933). Physical Review, 43, 103.

Bainbridge, K. T. (1933). Physical Review, 43, 1056.

Bainbridge, K.T. (1949). Physical Review, 75, 216A.

Bainbridge, K. T. (1953). Experimental Nuclear Physics, V. 1, ed. E. Segre, p.559. New York: Wiley.

Barber, R. C. (1965). Canadian Journal of Physics, 43, 716.

Barber, R. C., Duckworth, H. E. & Venkatasubramanian, V. (1983). Mass Spectroscopy, 2nd ed. (to be published)

Baril, M. and Kerwin, L. (1965). Canadian Journal of Physics,43, 716.

Barnard, G. P. (1953). Modern Mass Spectrometry, London: Unwin Brothers Ltd.

Bertrand, F. E. (1973). Nuclear Data Sheets, V.10, No. 2 91.

Birge, R. T. (1932). Physical Review, 40 207.

Bishop, R. L. (1969). Ph.D. Thesis, U. of Manitoba.

Bleakney, W. (1936). American Physics Teacher, 4, 12.

Coggshall, N. D. (1947). Journal of Applied Physics, 18, 855.

Dawson, P. H. (1976). Quadrupole Mass Spectrometry and its Applications. ed P. H. Dawson, Amsterdam, Oxford, New York: Elsevier.

Derenchuk, V. P. (1980). MSc. Thesis, U. of Manitoba.

Duckworth, H. E. (1958). Mass Spectroscopy. Cambridge:

Duckworth, H. E., (1957). Progress in Nuclear Physics, V.6 138.

Ellis, R. J. (1983). Ph.D. Thesis, U. of Manitoba.

Enge, H. A. (1964). Review of Scientific Instruments, 35, 278.

Enge, H., (1969). Introduction to Nuclear Physics. Reading, Menlo Park, London, Amsterdam, Sydney: Addison-Wesley.

Ezoe, H. (1970). Review of Scientific Instruments, 41, 952.

Goldstein, (1886). Berl. Ber. ,39, 691.

Halsted, R. E., (1952) Physical Review, V.88, No. 3, 666.

Herzog, R. (1934). Zeitschrift fur Physik, 89, 447.

Herzog, R. (1935). Zeitschrift fur Physik, 97, 596.

Herzog, R. (1955). Zeitschrift fur Naturforschung,10a, 855.

Hintenberger, H. and Konig, L. A. (1959). Advances in Mass Spectrometry, V. 1, ed. Waldron, J. D., P. 16 London, Paris, New York: Pergamon Press.

Kaufman, (1901). Phys. Z, 2, 602.

Konig, L. A. and Hintenberger, H. (1955). Zeitschrift fur Naturforschung, 10a, 877.

Kozier, K. S. (1977). Ph.D. Thesis, U. of Manitoba.

Kozier, K. S., Sharma, K. S., Barber, R. C., Barnard, J. W, Ellis, R.J., Derenchuk, V. P., and Duckworth, H. E. (1979). Canadian Journal of Physics,V. 57, No. 2, 266.

Maripuu, S. (1975). Atomic Data and Nuclear Data Tables, 17, No. 5-6.

Matsuda, H., (1961). The Review of Scientific Instruments, V. 32, No. 7, 850.

Matsuo, T., Matsuda, H. and Wollnik, H. (1972). Nuclear Instruments and Methods 103, 515.

Mattauch, J. (1960). Proceedings of the international conference on Nuclidic Masses, ed. Duckworth H. E., Toronto: Univ. of Tornto Press, p.3.

Meredith, J. O. (1971). Ph.D. Thesis, U. of Manitoba.

Merrihue, C. M., (1961). Physical Review,V. 124, No. 1, 208.

Meyerhof, W. E., Elements of Nuclear Physics,, New York, San Francisco, St. Louis, Toronto, London, Sydney:McGraw-Hill.

Nier, A. O. and Roberts, T. R., (1951) Physical Review, V. 81, No. 4, 507.

Ploch, W. and Walcher, W. (1950). Zeitschrift fur Physik, 127, 274.

Primakoff, H. and Rosen, S. P. (1959). Reports on Progress in Physics, XXII, 121.

Reutersward, C. (1951). Arkiv for Fysik,3, 53.

Reutersward, C. (1952). Arkiv for Fysik,4, 159.

Sharma, K. S. (1979). Ph.D. Thesis, U. of Manitoba.

Sharma, K. S., Ellis, R. J., Derenchuk, V. P. and Barber, R. C., and Duckworth, H. E., (1980). Physics Letters, V.91B, No. 2, 211.

Smith, L. G., (1952). Physical Review, 85, 767.

Southon, F.C.G. (1973). Ph. D. Thesis, U of Manitoba.

Standing, K. G., Chait, B. T., Ens, W., McIntosh, G. and Beavis, R. (1982). Nuclear Instruments and Methods, 198, 33-38, 33.

Swann, W. F. G. (1931). J. Franklin Inst., 212, 439.

Thomson, J. J. (1913). Rays of Positive Electricity: Longmans Green and Company.

Von Ardenne, M.. (1962). Tabellen zur Angewandten Physik, Band 1 (veb Deutscher Verlagder Wissenschaften, Berlin)

Wapstra, A. H. and Gove, N. B. (1971). The 1971 Atomic Mass Evaluation Nuclear Data Tables, ed. Katherine Way.

Wapstra, A. H. & Bos. K. (1977). Atomic Data and & Nuclear Data Tables, 1977 Atomic Mass Evaluation 19, No.1, 3 & 4.